



PRACTICAL COLLAPSE ASSESSMENT FOR REINFORCED CONCRETE STRUCTURES BASED ON SEISMIC RESPONSE SPECTRUM

Kazuto MATSUKAWA¹, Masaki MAEDA²

ABSTRACT: The collapse assessment of reinforced concrete (RC) structures is critical for evaluating their seismic capacity. In the past, the incremental dynamic analysis (IDA) method was used to assess the collapse. However, despite its accuracy, engineers avoid the IDA method because it is time-consuming. In this study, the authors used the method based on capacity spectrum method (CSM), which is more practical, to calculate the collapse limit and evaluate the seismic capacity of RC buildings. Finally, the authors compared the collapse limits evaluated by the CSM and IDA methods using observed and artificial ground motions. The results of both methods were in good agreement. In addition, it was found that the shape of the response spectrum affected the accuracy.

Key Words: *Collapse Assessment, Capacity Spectrum Method, Seismic Response Spectrum*

INTRODUCTION

Strong earthquakes may cause reinforced concrete structures to totally collapse owing to shear failure because of rapid degradation of their horizontal and axial capacity. In the Japanese seismic code and design standards, deterioration of shear resistance has not been considered because of its complexity and unclearness of calculation. Therefore, the safety limit state of building structures, which is the maximum displacement point of structures, is generally taken as the first occurrence of shear failure of a structural member. The safety limit is often a conservative estimate compared to actual collapse limit.

Structural engineers need to know the collapse limit displacement to calculate the actual seismic capacity of buildings. Therefore, the collapse risk needs to be assessed and is actively pursued by many research groups. For example, the collapse risk of structures designed according to the ASCE 7 (ASCE 2002, 2005) and ACI 318 standards was assessed using the incremental dynamic analysis (IDA) method (Haselton et. al. 2011, Liel et. al. 2011). In the IDA method, the ground motions are increasingly scaled and used as input until the structure collapse. However, a structural engineer who uses the IDA method needs to be knowledgeable and experienced and know how to perform time-consuming calculations; therefore, the method is not practical.

In this study, the authors evaluated the collapse limit of structures using the method based on the capacity spectrum method (CSM), which is a more practical method than IDA method. For that purpose, the authors confirm the accuracy of the collapse limit evaluation according to the CSM-based method by comparing it to the IDA-based method using SDOF system.

¹ Research associate

² Professor, Tohoku University

Most part of this paper was presented at 10th U.S. National Conference of Earthquake Engineering, Anchorage, Alaska July 21-25, 2014.

EVALUATION METHODOLOGY

IDA-based method

As shown in Figure 1, the IDA-based collapse limit evaluation consists of four steps. First, a set of ground motions with incrementally increasing amplitude scales (shown as “a”, “b” and “c”) is prepared. Second, a structural system that demonstrates capacity degradation after shear failure is determined (although simple SDOF model shown in Figure 1 is used in this study, using a frame model, an FEM model and another kind of a more detailed structural system is preferred for more accurate result.). Third, the set of ground motions is inputted to the structural system as shown in Figure 1 and the maximum response displacements (shown as “A” and “B”) are obtained, respectively. This process is called “incremental dynamic analysis”. When the amplitude scale of the ground motion is much higher than the capacity of the structural system, the system will collapse, as shown in step 3 in Figure 1. Collapse is defined as the appearance of dynamic instability in computations (same as past research (Haselton et. al. 2011, Liel et. al. 2011)). In addition, a collapse that occurs only in the horizontal direction, typically called the “side-sway collapse,” is considered in this study, but a collapse that occurs in the vertical direction, which occurs because of reduction in the axial capacity owing to shear failure of the column, is not considered.

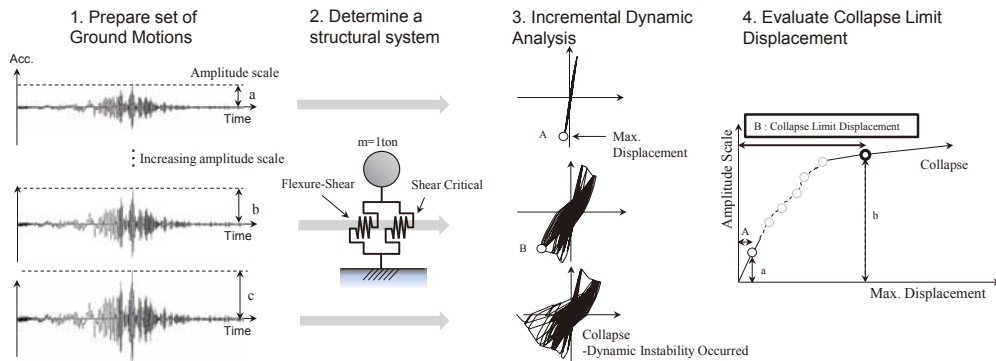


Figure 1 The IDA-based method procedure.

Finally, the relation of the amplitude scale and the maximum displacement is used to evaluate the collapse limit displacement, as shown in Figure 1. The maximum response displacement for the maximum amplitude scale of the ground motion at which the structural system does not collapse is taken as the collapse limit displacement. This is shown as point B in Figure 1.

CSM-based method

The key features of the CSM-based evaluation of the collapse limit against the side-sway collapse proposed by the authors (Matsukawa et. al. 2012) are summarized as follows:

- 1) Calculate the seismic capacity index (SCI (AIJ. 2004)) for the equivalent SDOF system, which is typically converted from the frame model using nonlinear static analysis.
- 2) Consider the maximum SCI point of the equivalent SDOF system as the collapse limit.

SCI is defined as the ratio of spectral acceleration of the ultimate spectrum at each response point on the capacity curve (5% damping, Lu, as shown in Figure 2) and the spectral acceleration of the standard spectrum (5% damping, Ls) at the period of each response point, as shown in Figure 2. The ultimate spectrum at each response point on the capacity curve is defined as the 5% damping response spectrum that its demand spectrum intersects the response point on the capacity curve (point A in Figure 2). Therefore, the SCI increments will roughly correspond with amplitude scale of IDA (see Figure 3). Similarly to the IDA-based method, the maximum SCI point is taken as the collapse limit displacement, which denotes the maximum response point at which the structure does not collapse for the maximum resistible scaled ground motion.

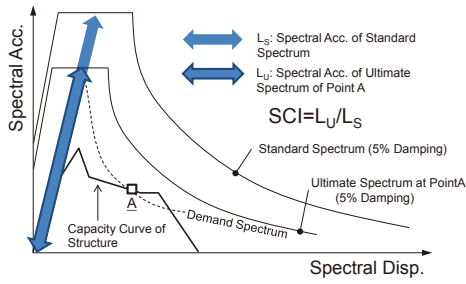


Figure 2 General concept of SCI.

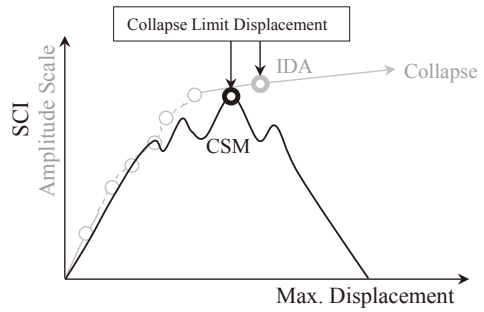


Figure 3 Relation of SCI and the amplitude scale of IDA.

Analytical Models and Ground Motions

The SDOF system, which consists of a mass (1 ton) with two shear springs in parallel, is used in this study (Figure 1). Each shear spring is applied backbone characteristics to show the shear critical member and flexural shear member, respectively. As shown in Figure 5, the spring which behaves as shear critical member is called “spring S” and the other spring is called “spring F”.

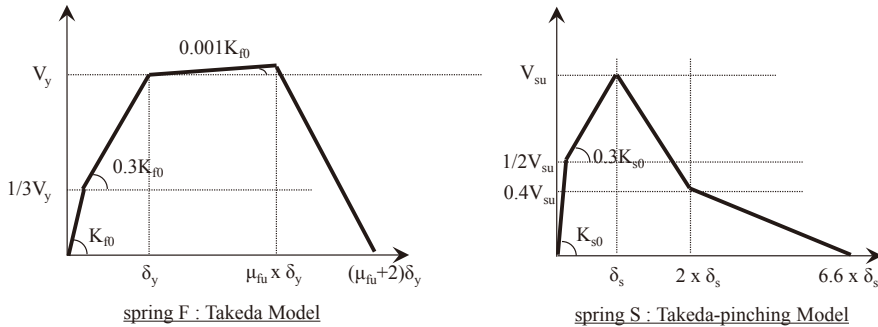


Figure 4 Backbone characteristics of each shear spring.

The parameters of the SDOF system are natural period ($T=0.2-0.8\text{sec}$), μ_{fu} (see Figure 5, $\mu_{fu}=2, 3$ and 4) and the maximum strength ratio of both shear springs (spring S: spring F=1:1, 1:2). The maximum strength of each spring is shown as V_y and V_{su} in Figure 4 and is determined by the maximum strength ratio. The summation of V_y and V_{su} are determined to be 0.6 of base shear coefficient. Table1 shows the parameters for each spring and overall systems for an example (S:F=1:1).

The hysteresis behavior proposed in (Takeda et.al 1970) is used in each spring. For spring S, Takeda-pinching model is applied to consider effect of the deterioration of the bonding strength between the steel bars and concrete. For spring F, pinching is not considered in the hysteresis loop for demonstrating the large energy absorption.

Table 1 Parameters for each spring and overall system.

	unit	0.2sec		0.3sec		0.4sec		0.5sec		0.6sec		0.7sec		0.8sec	
		S	F	S	F	S	F	S	F	S	F	S	F	S	F
Disp. at $1/3V_s(V_s)$	cm	0.2	0.2	0.4	0.4	0.7	0.7	1.1	1.1	1.6	1.6	2.2	2.2	2.9	2.9
$1/3V_s(V_s)/\text{Weight}$	-	0.09	0.09	0.09	0.09	0.09	0.09	0.09	0.09	0.09	0.09	0.09	0.09	0.09	0.09
δ_v	cm	1.0	1.6	2.3	3.5	4.1	6.3	6.3	9.8	9.1	14.1	12.4	19.2	16.2	25.1
$V_s(V_s)/\text{Weight}$	-	0.30	0.30	0.30	0.30	0.30	0.30	0.30	0.30	0.30	0.30	0.30	0.30	0.30	0.30
Max Capacity of System	-	0.51		0.51		0.51		0.51		0.51		0.51		0.51	
$\mu_{hi} \times \delta_v$: ($\mu_{hi}=2$)	cm	-	3.1	-	7.1	-	12.6	-	19.6	-	28.3	-	38.5	-	50.3
$\mu_{hi} \times \delta_v$: ($\mu_{hi}=3$)	cm	-	4.7	-	10.6	-	18.8	-	29.4	-	42.4	-	57.7	-	75.4
$\mu_{hi} \times \delta_v$: ($\mu_{hi}=4$)	cm	-	6.3	-	14.1	-	25.1	-	39.3	-	56.5	-	77.0	-	100.5
$(\mu_{hi}+2)\delta_v$: ($\mu_{hi}=3$)	cm	6.8	7.9	15.2	17.7	27.0	31.4	42.2	49.1	60.8	70.7	82.8	96.2	108.1	125.6
Disp at capacity of system = 0: ($\mu_{hi}=3$)	cm	7.9		17.7		31.4		49.1		70.7		96.2		125.6	

A set of ground motions is consists of twelve observed ground motions (observed at 6 stations, both NS (N) and EW (E) directions are included) and ten artificial ground motions; Elcentro wave (EL_N and EL_E), Kobe wave (KB_N and KB_E), Hachinohe wave (HC_N and HC_E), Ojiya wave (OJ_N and OJ_E), Taft wave (TF_N and TF_E), Tohoku wave (TH_N and TH_E) and ten artificial waves which are made to fit response spectrum indicated in Japanese building code (soil type2). The artificial ground motions are shown in Figure 5. The five artificial ground motions with a duration of 30sec are called S series and the other five artificial ground motions with a duration of 120 sec are called LL series. Each ground motions is marked as “LL05” or “S03”, respectively. The calculated response spectrum using the artificial ground motions and target spectrum are shown in Figure 6.

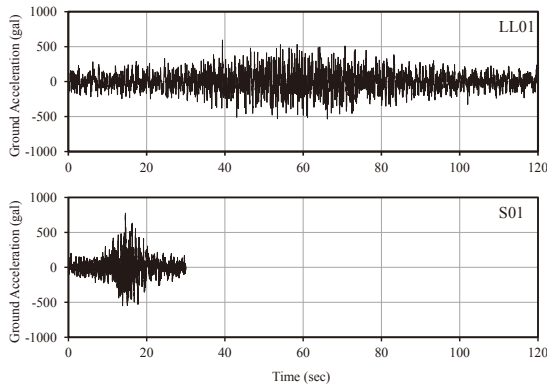


Figure 5 Acceleration time series of artificial ground motions.

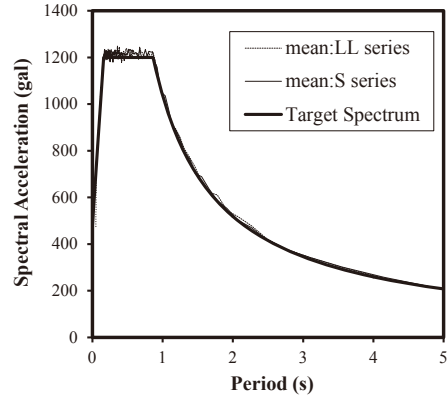


Figure 6 Averaged spectral acceleration of each series of artificial ground motions.

Consideration of Asymmetrical Behavior

To compare the CSM and IDA methods, it is important to discuss the effect of asymmetrical behavior that is observed during the dynamic analysis, where the maximum response displacement in the positive and negative direction is significantly different, as shown in Figure 7. The equivalent period commonly used in the CSM is calculated by equivalent stiffness at the maximum response point - if the equivalent mass is constant - even though substantial equivalent period is significantly shorter. This is caused because the typical assumptions in the CSM are steady response and symmetrical behavior. In addition, the energy absorption owing to the hysteresis loop (damping) will decrease because of the asymmetrical behavior in Figure 8.

To consider the effect of asymmetrical behavior, the symmetrical ratio β and adjusting factor of equivalent period α_T (Okano et.al 2012) are defined in Equation (1) and (2), respectively. The corresponding variabilities are shown in Figures 7 and 8.

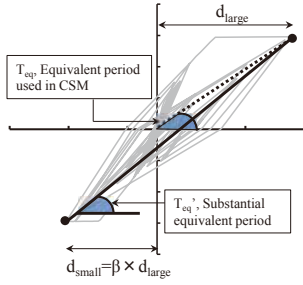


Figure 7 Asymmetrical behavior of dynamic analysis.

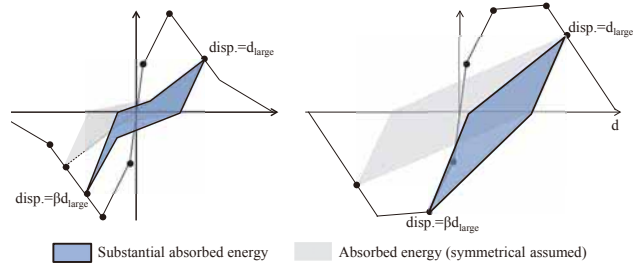


Figure 8 Hysteresis loop assumption using β .

$$\beta = d_{small} / d_{large} \quad (1)$$

$$\alpha_T = T_{eq}' / T_{eq} \quad (2)$$

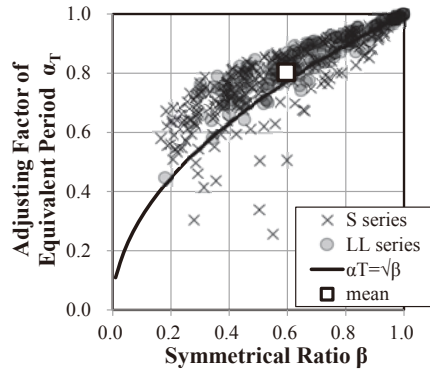


Figure 9 α_T versus β at collapse limit calculated by the IDA-based method.

The values at collapse limit are calculated from results of the IDA-based method using the artificial waves. Figure 9 shows the calculated values of α_T and β by Equation (1) and (2), at the collapse limit. The black line in Figure 10 is mathematical values when bi-linear characteristic assumed. The average values for α_T and β are 0.80 and 0.60, respectively, and they are taken into the CSM calculations.

The damping ratio h_{eq} of structural system is calculated as weighted average of the damping factor of each spring by using their potential energy. Viscous and hysteresis damping of each spring are included in h_{eq} . The initial viscous damping is assumed as 5% and the hysteresis damping is calculated as the ratio of absorbed and potential energies.

β is considered in the hysteresis damping calculations, as shown in Figure 8. In addition, reduction factor for calculating the demand spectrum shown in Figure 2, F_h is calculated by Equation (3) and is multiplied to standard spectrum (5% damping) for calculation of demand spectrum.

$$F_h = \frac{1.5}{1 + 10h_{eq}} \quad (3)$$

ANALYTICAL RESULTS

Results for the Artificial Ground Motions

The collapse limit calculated by both methods for artificial ground motions is compared. Figure 10 shows the results of the collapse limit evaluation by both methods and the collapse limit point on the capacity curve of the structures. Figure 11 shows the amplitude scale of the input ground motion. From Figure 11, it is found that even though the amplitude scale calculated by the CSM-based method is underestimated relative to the results of IDA-based method, the collapse limit point evaluated by using both methods is in good agreement.

The collapse limit displacement and amplitude scale (SCI) calculated by the CSM-based method were divided by the collapse limit displacement and amplitude scale calculated by the IDA-based method and plotted in the vertical axis of Figures 12 (a) and (b), respectively. In addition, they are averaged and arranged for each ground motion and natural period of each structural system. The collapse limit displacement in Figure 12 (a) shows the validity of the CSM-based evaluation with an average error of $\pm 20\%$ and an average relative accuracy (vertical axis) of nearly 1.0 although the amplitude scale is underestimated.

The effect of duration time can be found from the results. The collapse limit displacement for the S series of ground motions are of higher accuracy than the LL series ground motions with values near 1.0 in Figure 12 (a). In addition, structural system with short natural period (such as $T=0.2\text{sec}$, 0.3 sec , etc. denoted by the open symbols in Figure 12 (a)) shows large variability, which is related to the capacity degradation curve of such structural systems and it will be discussed in detail in the near future.

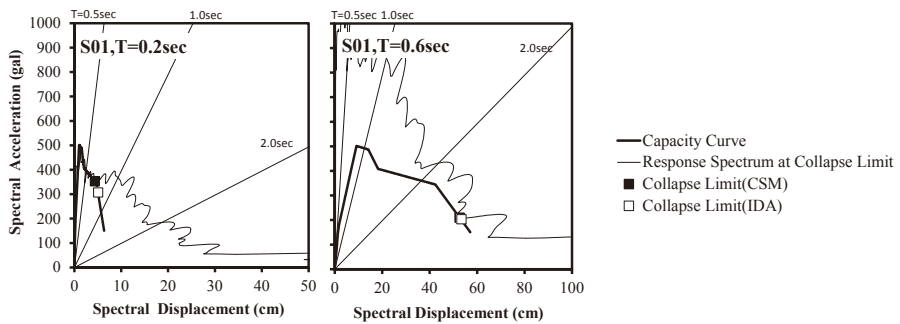


Figure 10 Examples of collapse limit evaluation.

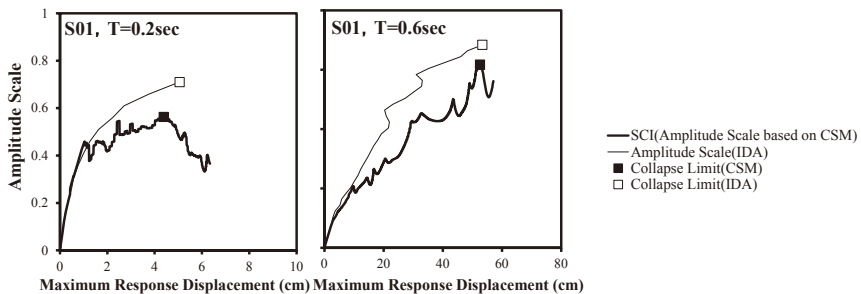


Figure 11 Amplitude scale of the input ground motion.

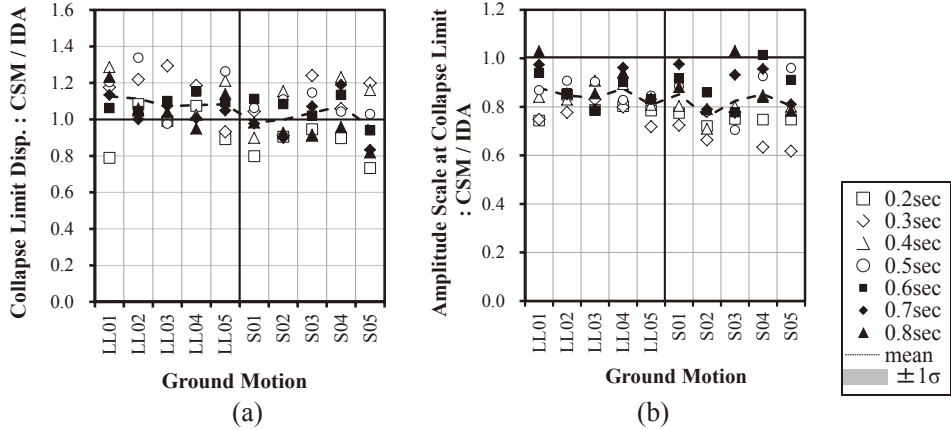


Figure 12 Accuracy of the collapse limit evaluation for artificial ground motions.

Substitute damping factor, h_s , which is derived from IDA analysis, calculated by Equation (4) is taken to know the validity of h_{eq} used in CSM-based method. h_{eq} which used in CSM-based method is compared with h_s in Figure 13. At results, increment of h_{eq} evaluated using Figure 8 was good agreement with increment of h_s .

$$h_s = -\int_0^t \ddot{y}_0 \dot{y} dt / \left(2\omega \int_0^t \dot{y}^2 dt \right) \quad (4)$$

Where, \ddot{y}_0 and \dot{y} are ground acceleration and response velocity, respectively. ω is fundamental angular frequency.

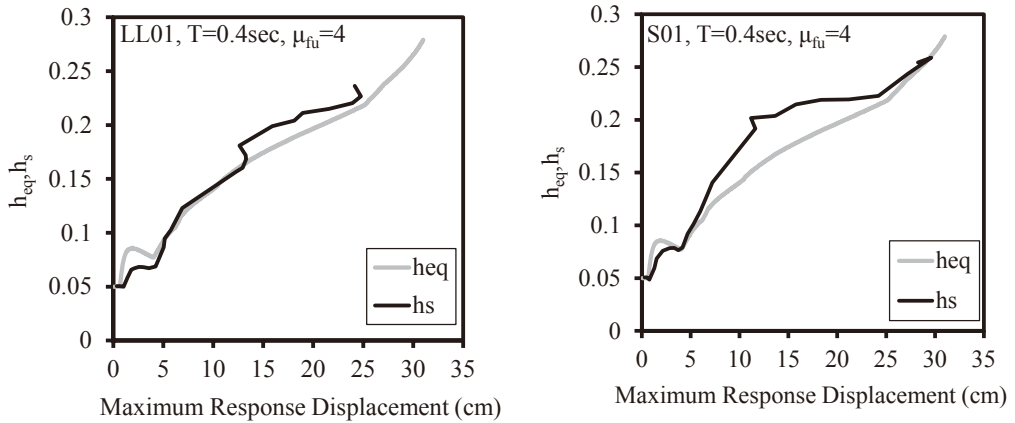


Figure 13 h_s (substitute damping factor) and h_{eq}

Results for Observed Ground Motion

In this chapter, analytical results for observed ground motions are shown. Response spectrum calculated by the observed ground motion has strong unevenness shape, which would possibly affect SCI and collapse limit, as shown in Figure 14.

The correspondence among the evaluation results by both methods is relatively good (Figure 15

(a)); however, a relatively large error in the collapse limit evaluation is shown in Figure 15 (b). As shown in Figure 15(a), the SCI is affected by unevenness of the response spectrum. The unevenness clarifies the SCI peak; therefore, it is possible to obtain accurate and reliable results by the CSM-based method. In contrast, although the unevenness clarifies the SCI peaks, large errors could be found in the examples shown in Figure 15 (b). The cause of such results could be explained by differences in each SCI peak. The difference of each SCI peak is relatively small in example shown in Figure 15 (b), therefore, clearly, such differences affect the accuracy.

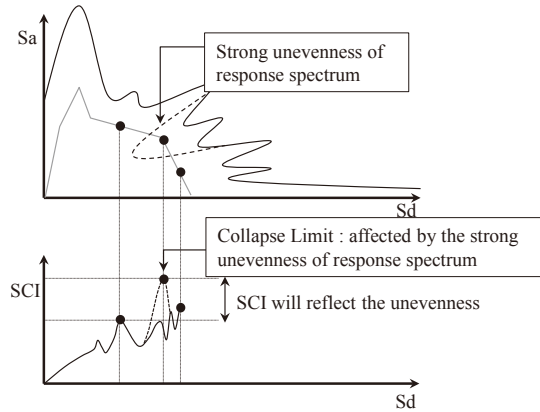


Figure 14 Unevenness of the spectrum shape and its relation to SCI.

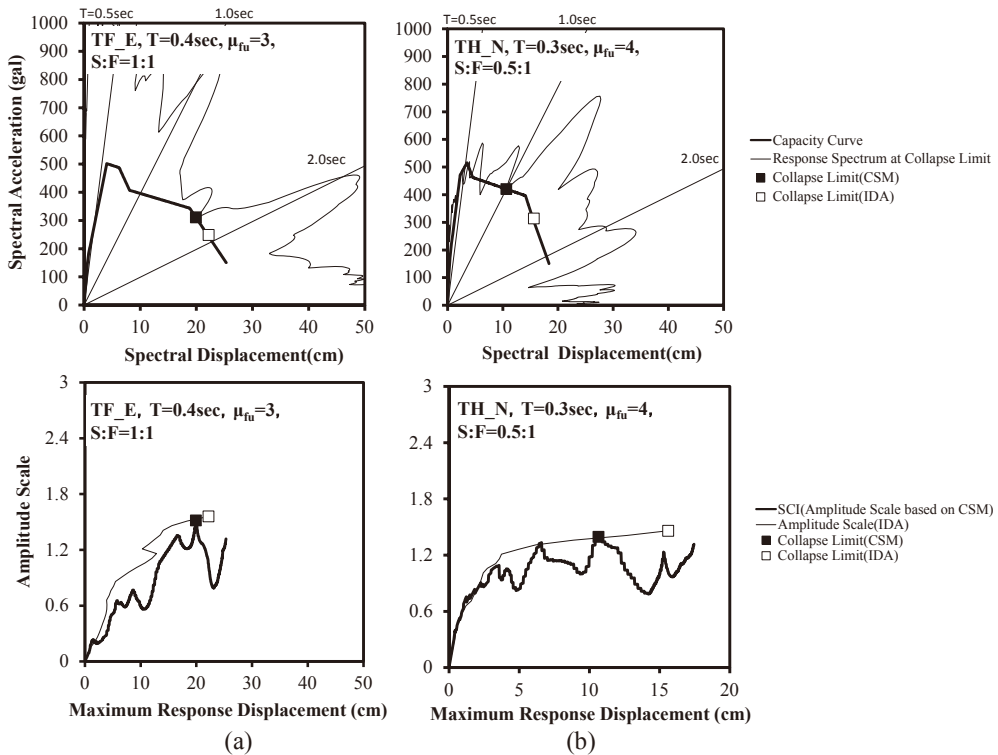


Figure 15 Examples of the collapse limit evaluation for the observed ground motions.

Figure 16 shows the accuracy of the collapse limit displacement (Figure 16 (a)) and amplitude scale at the collapse limit (Figure 16 (b)). Although the accuracy of the collapse limit displacement by the CSM-based method is highly variable compared to the results for the artificial ground motions, the variability is due to the short natural period of the structural systems (Figure 16(a)). Actually, the standard deviation decreases from 0.30 to 0.19 if the results for the 0.2 s period are omitted.

The results suggest that the CSM-based method is well suited for evaluating the collapse limit displacement if observed ground motions are used, except for structural systems having short natural periods.

On the contrary, the evaluation of the amplitude scale at the collapse limit, as shown in Figure 16 (b), shows large variability even for structural systems with long natural periods. This suggests that although unevenness of response spectrum may help to evaluate the collapse limit displacement, the spectrum unevenness causes the amplitude scale between the IDA and CSM to differ.

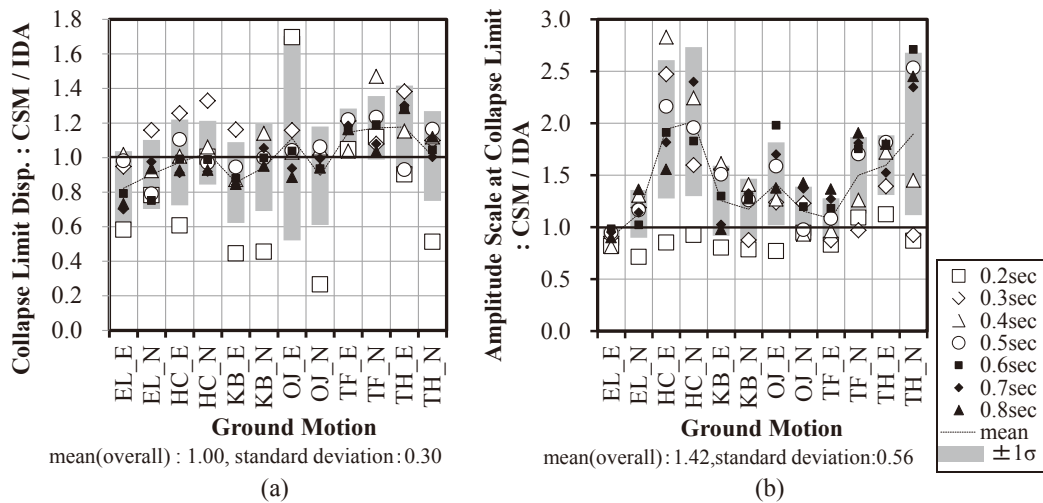


Figure 16 Accuracy of collapse limit evaluation.

CONCLUSIONS

Based on the above discussion, the authors conclude the following.

- 1) The CSM-based method for evaluating the collapse limit is valid and practical.
- 2) The collapse limit displacement evaluated by the CSM-based method is in good agreement with the IDA-based method except for structural systems with short natural periods. For artificial ground motions, the errors are approximately within $\pm 20\%$.
- 3) Ground motions with duration of 30 s and 120 s were used in assessing the collapse. The differences in the duration time affected the collapse limit displacement by 10%.
- 4) The unevenness in the shape of the response spectrum significantly affected the accuracy of the CSM-based method. Ground motions with large unevenness showed higher accuracy.

ACKNOWLEDGEMENTS

This work was supported by KAKENHI 23360238, a Grant-in-Aid for Scientific Research (B) to Masaki Maeda. The authors wish to thank all who assisted them in this research.

REFERENCES

- Curt B. Haselton, Abbie B. Liel, Gregory G. Deierlein, Brian S. Dean and Jason H. Chou (2011), "Seismic Collapse Safety of Reinforced Concrete Buildings. I: Assessment of Ductile Moment Frames." *Journal of Structural Engineering*, 481-491.
- Abbie B. Liel, Curt B. Haselton and Gregory G. Deierlein (2011), "Seismic Collapse Safety of Reinforced Concrete Buildings. II: Comparative Assessment of Nonductile and Ductile Moment Frames." *Journal of Structural Engineering*, 492-502.
- Kazuto Matsukawa, Masaki Maeda, Hamood Al-Washali and Kanako Takahashi (2012) "Research For Collapse of R/C Frame Composed of Shear And Flexure Column", *Proceedings of the 15th World Conference Earthquake Engineering*, paper No. 1501.
- Architectural Institute of Japan (2004), "*Guidelines for Performance Evaluation of Earthquake Resistant Reinforced Concrete Buildings (Draft)*" (in Japanese)
- Toshikazu Takeda., M. A. Sozen, and N. N. Nielsen (1970) "Reinforced Concrete Response to Simulated Earthquakes", *Proceedings of ASCE, Journal of Structural Division*, Vol.96, 2557-2573.
- Hajime Okano and Yuji Miyamoto (2012), "Equations Derived From Equivalent Linearization Method, Consideration based on energy balance and its application to evaluation of probability of excess of deformation capacity", *Journal of Structural and Construction Engineering (Transactions of AIJ)* (In Japanese), No.562, 45-52.